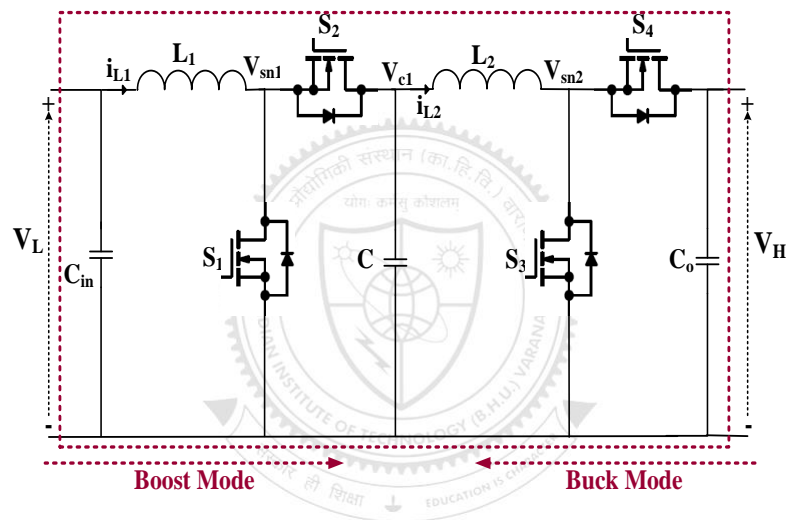
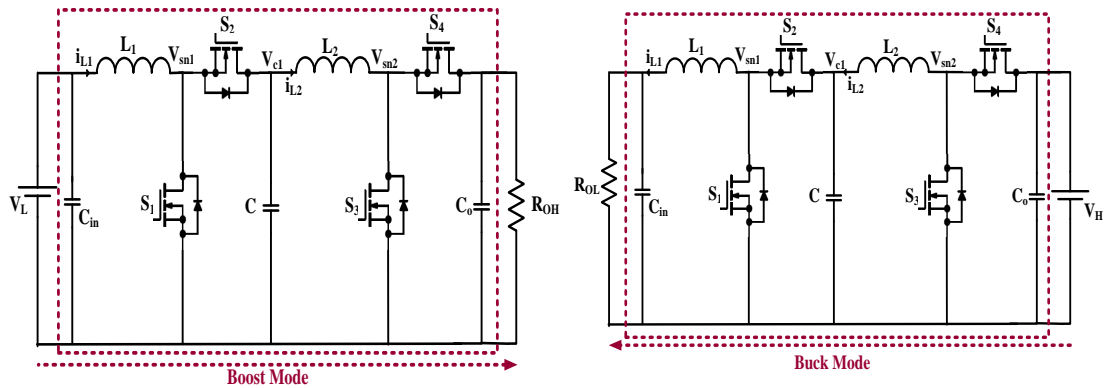


APPENDIX A

The proposed bidirectional quadratic converter is capable of bidirectional power flow. In this proposed quadratic converter both quadratic boost and quadratic buck operating modes are possible. The bidirectional converter is made by cascading two boost converters which makes it a quadratic boost converter. For making it bi-directional, the diodes are replaced by switches with body diodes. So, this converter behaves as a quadratic boost converter as well as a quadratic buck converter.



(a)



(b)

(c)

Fig. A. 1. (a) Proposed Bidirectional Quadratic Converter (b) Quadratic Boost mode of operation (c) Quadratic Buck mode of operation

A.1. Quadratic Boost Mode of Operations

Quadratic boost mode converter is shown in Fig. A.1 (b). In this mode, V_L is an input whereas R_{OH} is load resistance of the quadratic boost converter. Quadratic boost operation will be achieved when the switches S_1 and S_3 operate at the same duty cycle and same instant. When switches S_1 and S_3 turn-off, body diodes of the switches S_2 and S_4 are operated. In this mode of operation switches, S_2 and S_4 are always turned-off.

Perturbation and linearization of the differential equation leads to the following state space model in the quadratic boost mode of operations (fig. shown in A.1(b))

$$\frac{d}{dt} \begin{bmatrix} \hat{i}_{L1} \\ \hat{i}_{L2} \\ \hat{v}_c \\ \hat{v}_o \end{bmatrix} = [A] \times \begin{bmatrix} \hat{i}_{L1} \\ \hat{i}_{L2} \\ \hat{v}_c \\ \hat{v}_o \end{bmatrix} + [B]^T \times [\hat{V}_L] + [E]^T \times [\hat{d}],$$

$$A = \begin{bmatrix} 0 & 0 & \frac{-(1-D)}{L_1} & 0 \\ 0 & 0 & \frac{1}{L_2} & \frac{-(1-D)}{L_2} \\ \frac{1-D}{C} & \frac{-1}{C} & 0 & 0 \\ 0 & \frac{1-D}{C_0} & 0 & \frac{-1}{R_{OH}C_0} \end{bmatrix}$$

$$B = \begin{bmatrix} \frac{1}{L_1} & 0 & 0 & 0 \end{bmatrix} \text{ and } E = \begin{bmatrix} \frac{V_c}{L_1} & \frac{V_o}{L_2} & \frac{-I_{L1}}{C} & \frac{-I_{L2}}{C_0} \end{bmatrix}$$

The open loop control-to-output transfer function of the proposed converter can be derived as follows.

$$\frac{\hat{v}_o}{\hat{d}} = [0 \ 0 \ 0 \ 1 \ 0][sI - A]^{-1}[U_1] \quad (A.1)$$

Whereas, $U_1 = \begin{bmatrix} \frac{V_c}{L_1} & \frac{V_o}{L_2} & \frac{-I_{L1}}{C} & \frac{-I_{L2}}{C_0} \end{bmatrix}^T$.

By solving (A.1), the following open loop control to output transfer function is obtained as

$$G_{plant} = \frac{\hat{v}_o}{\hat{d}} = \frac{A_1 S^3 + B_1 S^2 + C_1 S + D_1}{A_2 S^4 + B_2 S^3 + C_2 S^2 + D_2 S + E_2} \quad (A.2)$$

The numerator and denominator coefficients of (A.2) are as follows:

$$A_1 = CL_1 L_2 V_o ,$$

$$B_1 = -CL_1 R_{oH} V_L ,$$

$$C_1 = (1 - D)^2 L_2 V_o + L_1 V_o ,$$

$$D_1 = -2R_{oH} V_L (1 - D)^2$$

$$A_2 = -(1 - D)CC_o L_1 L_2 R_{oH} ,$$

$$B_2 = -(1 - D)CL_1 L_2 ,$$

$$C_2 = -(1 - D)^2 R_{oH} (C_o L_2 + CL_1) + C_o L_1 R_{oH} (D - 1),$$

$$D_2 = -L_2 (1 - D)^3 + L_1 (D - 1) ,$$

$$E_2 = -R_{oH} (1 - D)^5 .$$

A.2. Quadratic Buck Mode of Operations

Fig. A.1 (c) shows the proposed converter operating in quadratic buck mode. In this mode, V_H is an input whereas R_{oL} is load resistance of the converter. Quadratic buck operation will be achieved when the switches S_2 and S_4 operate at the same instant and same duty cycle. Body diodes of the switches S_1 and S_3 are turned on when switches S_2 and S_4 turn-off. In this mode of operation, switches, S_1 and S_3 are always a turned-off.

Perturbation and linearization of the differential equation leads to following state space model in the quadratic buck mode of operations (fig. shown in A.1(c))

$$\frac{d}{dt} \begin{bmatrix} \hat{i}_{L2} \\ \hat{i}_{L1} \\ \hat{v}_c \\ \hat{v}_o \end{bmatrix} = [A] \times \begin{bmatrix} \hat{i}_{L2} \\ \hat{i}_{L1} \\ \hat{v}_c \\ \hat{v}_o \end{bmatrix} + [B]^T \times [\widehat{V}_H] + [E]^T \times [\hat{d}],$$

$$A = \begin{bmatrix} 0 & 0 & -\frac{1}{L_2} & 0 \\ 0 & 0 & \frac{D}{L_1} & -\frac{1}{L_1} \\ \frac{1}{C} & -\frac{D}{C} & 0 & 0 \\ 0 & \frac{1}{C_0} & 0 & -\frac{1}{R_{OL}C_0} \end{bmatrix}$$

$$B = \begin{bmatrix} \frac{D}{L_2} & 0 & 0 & 0 \end{bmatrix} \text{ and } E = \begin{bmatrix} \frac{V_H}{L_2} & \frac{V_c}{L_1} & \frac{-I_{L1}}{C} & 0 \end{bmatrix}$$

$$\frac{\hat{v}_o}{\hat{d}} = [0 \ 0 \ 0 \ 1][sI - A]^{-1}[U_1]$$

$$\text{Where } U_1 = \begin{bmatrix} \frac{V_H}{L_2} & \frac{V_c}{L_1} & \frac{-I_{L1}}{C} & 0 \end{bmatrix}^T$$

$$G_{plant} = \frac{\hat{v}_o}{\hat{d}} = \frac{A_3s^2 + B_3s + C_3}{A_4s^4 + B_4s^3 + C_4s^2 + D_4s + E_4} \quad (\text{A.3})$$

Whereas,

$$A_3 = CDL_2R_{OL}V_H, B_3 = -DL_2R_{OL}I_{L1}, C_3 = 2DR_{OL}V_H$$

$$A_4 = CC_0L_2L_1R_{OL}, B_4 = C_0L_2R_{OL}D^2 + CL_2R_{OL} + C_0L_1R_{OL}$$

$$C_4 = CL_2L_1, D_4 = L_1 + L_2D^2, E_4 = R_{OL}$$

Bode plot of control-to-output transfer function of quadratic boost mode and quadratic buck mode is given in Fig. A. 2. The components values are taken as $L_1=310\mu\text{H}$, $L_2=360\mu\text{H}$, $C_0=100\mu\text{F}$, $C_{in}=100\mu\text{F}$, $C=47\mu\text{F}$ for 100 kHz switching frequency. Same components are used for both the modes of operations.

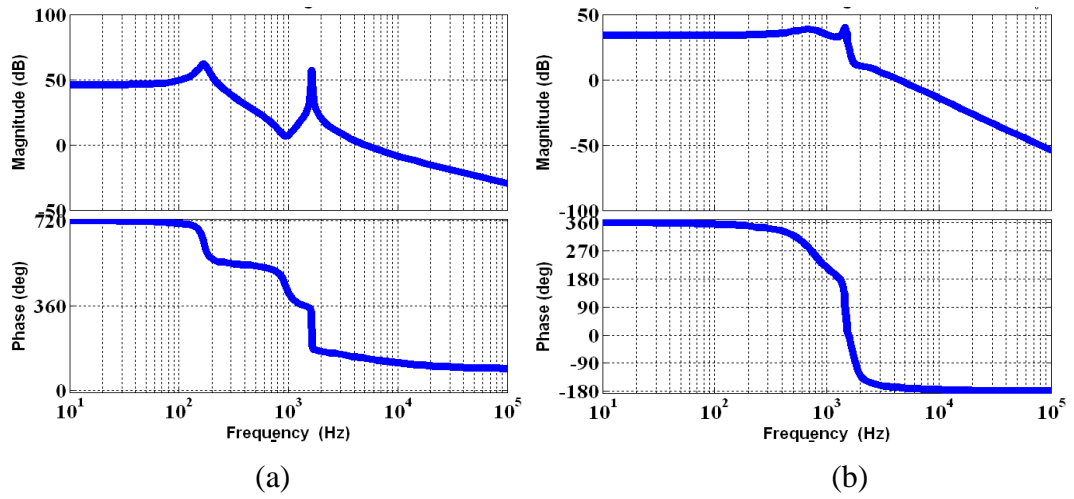


Fig. A. 2. Bode plots of control to output transfer function of (a) Quadratic Boost mode of operation (b) Quadratic Buck mode of operation





APPENDIX B

The two conventional boost converters are cascaded and diodes are replaced by bidirectional switches. By doing this a bi-directional converter is achieved and both quadratic boost and quadratic buck mode operation is possible. The proposed bi-directional converter consists of magnetically coupled inductor and a damping network. With this arrangement, right-half-plane (RHP) zero for the quadratic boost mode of operation is completely eliminated and the converter becomes capable of handling large ripple currents in quadratic buck mode of operations. Proposed coupled inductor based bidirectional converter is shown in Fig. B.1(a)

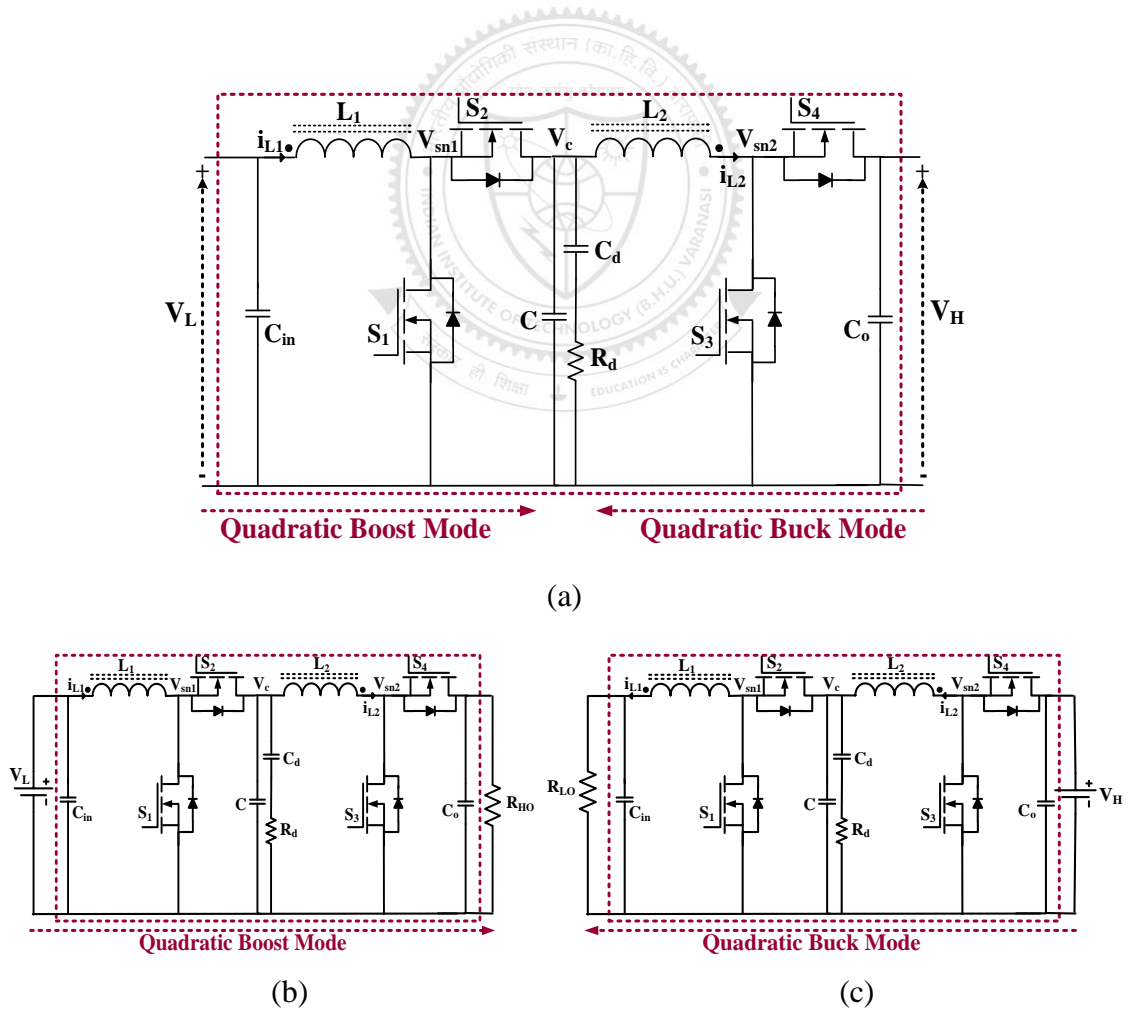


Fig. B. 1. (a) Proposed Coupled inductors Bidirectional Quadratic Converter (b) Quadratic Boost mode of operation (c) Quadratic Buck mode of operation.

B.1. Quadratic Boost Mode of Operations

The quadratic boost mode operation of the proposed converter is shown in fig. B. 1 (b). In this mode, V_L is an input whereas R_{OH} is load resistance of the proposed quadratic boost converter. Quadratic boost operation will be achieved when switches S_1 and S_3 operate at the same duty cycle and the same instant. When switches S_1 and S_3 turn-off body diodes of the switches S_2 and S_4 are operated. In this mode of operation switches, S_2 and S_4 are always a turned-off.

Purturbation and linearization of the differential equation leads to following state space model in the quadratic boost mode of operation. (Fig. shown in B.1(b))

$$\frac{d}{dt} \begin{bmatrix} \hat{i}_{L1} \\ \hat{i}_{L2} \\ \hat{v}_c \\ \hat{v}_o \\ \hat{v}_d \end{bmatrix} = [A] \times \begin{bmatrix} \hat{i}_{L1} \\ \hat{i}_{L2} \\ \hat{v}_c \\ \hat{v}_o \\ \hat{v}_d \end{bmatrix} + [B]^T \times [\widehat{V}_{in}] + [E]^T \times [\hat{d}] ,$$

$$A = \begin{bmatrix} 0 & 0 & \frac{M + DL_2 - L_2}{L_1L_2 - M^2} & \frac{DM - M}{L_1L_2 - M^2} & 0 \\ 0 & 0 & \frac{L_1 + DM - M}{L_1L_2 - M^2} & \frac{DL_1 - L_1}{L_1L_2 - M^2} & 0 \\ \frac{1-D}{C} & \frac{-1}{C} & \frac{-1}{R_dC} & 0 & \frac{1}{R_dC} \\ 0 & \frac{1-D}{C_0} & 0 & \frac{-1}{R_0C_0} & 0 \\ 0 & 0 & \frac{1}{R_dC_d} & 0 & \frac{-1}{R_dC_d} \end{bmatrix}$$

$$B = \begin{bmatrix} \frac{L_2}{L_1L_2 - M^2} & \frac{M}{L_1L_2 - M^2} & 0 & 0 & 0 \end{bmatrix},$$

$$E = \begin{bmatrix} \frac{L_2V_c + MV_0}{L_1L_2 - M^2} & \frac{MV_c + L_1V_0}{L_1L_2 - M^2} & \frac{-I_{L1}}{C} & \frac{-I_{L2}}{C_0} & 0 \end{bmatrix}$$

The open loop control-to-output transfer function of the prospoed converter can be derived as follows.

$$\frac{\hat{v}_o}{\hat{d}} = [0 \ 0 \ 0 \ 1 \ 0][sI - A]^{-1}[U_1] \quad (\text{B.1})$$

Whereas,
$$U_1 = \left[\frac{L_2V_c + MV_0}{L_1L_2 - M^2} \quad \frac{MV_c + L_1V_0}{L_1L_2 - M^2} \quad \frac{-I_{L1}}{C} \quad \frac{-I_{L2}}{C_0} \quad 0 \right]^T.$$

By solving (B.1), the following open loop control to output transfer function is obtained

$$G_{plant} = \frac{\hat{v}_o}{\hat{d}} = \frac{A's^4 + B's^3 + C's^2 + D's + E'}{A''s^5 + B''s^4 + C''s^3 + D''s^2 + E''s + F''} \quad (\text{B.2})$$

The numerator and denominator coefficients of (B.2) are as follows:

$$A' = CC_d I_{L2} R_0 R_d (M^2 - L_1 L_2),$$

$$B' = I_{L2} R_0 (C + C_d) (M^2 - L_1 L_2) + CC_d R_0 R_d (1 - D) (L_1 V_0 + MV_c)$$

$$C' = C_d R_0 R_d \{ (I_{L1} M - I_{L2} L_2) (1 - D)^2 + (2I_{L2} M - I_{L1} L_1) (1 - D) \} \\ + R_0 (C + C_d) (L_1 V_0 + MV_c) (1 - D) - C_d R_0 R_d I_{L2} L_1$$

$$D' = C_d R_0 R_d V_0 (1 - D)^3 + R_0 (I_{L1} M - I_{L2} L_2 + C_d R_d V_c) (1 - D)^2 \\ + R_0 (2I_{L2} M - I_{L1} L_1) (1 - D) - I_{L2} L_1 R_0$$

$$E' = R_0 V_0 (1 - D)^3 + R_0 V_c (1 - D)^2;$$

$$A'' = CC_0 C_d R_0 R_d (L_1 L_2 - M^2),$$

$$B'' = (CC_0 R_0 + C_0 C_d R_0 + CC_d R_d) (L_1 L_2 - M^2)$$

$$C'' = (C + C_d) (L_1 L_2 - M^2) + C_d R_0 R_d (CL_1 + C_0 L_2) (1 - D)^2 - 2C_0 C_d R_0 R_d M (1 - D) \\ + C_0 C_d R_0 R_d L_1,$$

$$D'' = R_0 (C_d L_1 + C_0 L_2 + CL_1) (1 - D)^2 + C_d L_2 R_d (1 - D)^2 \\ - (C_0 R_0 + C_d R_d) (2M(1 - D) - L_1)$$

$$E'' = C_d R_0 R_d (1 - D)^4 + L_2 (1 - D)^2 - 2M(1 - D) + L_1,$$

$$F'' = R_0 (1 - D)^4$$

B.2. Quadratic Buck Mode of Operations

Fig. B. 1 (c) shows the quadratic buck mode operation of the proposed converter. In this mode, V_H is an input whereas R_{OL} is load resistance of the proposed quadratic buck converter. Quadratic buck operation will be achieved when the switches S_2 and S_4 operate at the same instant and same duty cycle. Body diodes of the switches S_1 and S_3 are turned on when switches S_2 and S_4 turn-off. In this mode of operation switches, S_1 and S_3 are always a turned-off.

Perturbation and linearization of the differential equation leads to following state space model in the buck mode of operation (Fig. shown in B.1(c))

$$\frac{d}{dt} \begin{bmatrix} \hat{i}_{L2} \\ \hat{i}_{L1} \\ \hat{v}_c \\ \hat{v}_o \\ \hat{v}_d \end{bmatrix} = [A] \times \begin{bmatrix} \hat{i}_{L2} \\ \hat{i}_{L1} \\ \hat{v}_c \\ \hat{v}_o \\ \hat{v}_d \end{bmatrix} + [B]^T \times [\widehat{V}_H] + [E]^T \times [\hat{d}],$$

Whereas, $A = \begin{bmatrix} 0 & 0 & \frac{MD-L_1}{(L_1L_2-M^2)} & \frac{-M}{L_1L_2-M^2} & 0 \\ 0 & 0 & \frac{L_2D-M}{L_1L_2-M^2} & \frac{-L_2}{L_1L_2-M^2} & 0 \\ \frac{1}{C} & \frac{-D}{C} & \frac{-1}{R_dC} & 0 & \frac{1}{R_dC} \\ 0 & \frac{1}{C_{in}} & 0 & \frac{-1}{R_{OL}C_{in}} & 0 \\ 0 & 0 & \frac{1}{R_dC_d} & 0 & \frac{-1}{R_dC_d} \end{bmatrix}$

$$B = \begin{bmatrix} \frac{L_1D}{L_1L_2-M^2} & \frac{MD}{L_1L_2-M^2} & 0 & 0 & 0 \end{bmatrix},$$

$$E = \begin{bmatrix} \frac{L_1V_H + V_C M}{L_1L_2 - M^2} & \frac{L_2V_C + MV_H}{L_1L_2 - M^2} & \frac{-I_{L1}}{C} & 0 & 0 \end{bmatrix}$$

$$\frac{\hat{v}_o}{\hat{d}} = [0 \quad 0 \quad 0 \quad 1][sI - A]^{-1}[U_1],$$

$$\text{Where } U_1 = \begin{bmatrix} \frac{L_1V_H + V_C M}{L_1L_2 - M^2} & \frac{L_2V_C + MV_H}{L_1L_2 - M^2} & \frac{-I_{L1}}{C} & 0 & 0 \end{bmatrix}^T$$

$$G_{plant} = \frac{\hat{v}_o}{\hat{d}} = \frac{A_3S^3 + B_3S^2 + C_3S + D_3}{A_4S^5 + B_4S^4 + C_4S^3 + D_4S^2 + E_4S + F_4} \quad (B.3)$$

Whereas,

$$A_3 = CC_dR_dR_{0L}(L_2V_C + MV_H),$$

$$B_3 = (C + C_d)(L_2R_{0L}V_C + MR_{0L}V_H) + C_dR_dR_{0L}I_{L1}(M - DL_2),$$

$$C_3 = (R_dR_{0L}C_d)(V_C + DV_H) + R_{0L}I_{L1}(M - DL_2),$$

$$D_3 = R_{0L}(V_C + DV_H)$$

$$A_4 = CC_{in}C_dR_dR_{0L}(L_1L_2 - M^2),$$

$$B_4 = (L_1L_2 - M^2)(C_dC_{in}R_{0L} + R_{0L}CC_{in} - CC_dR_d),$$

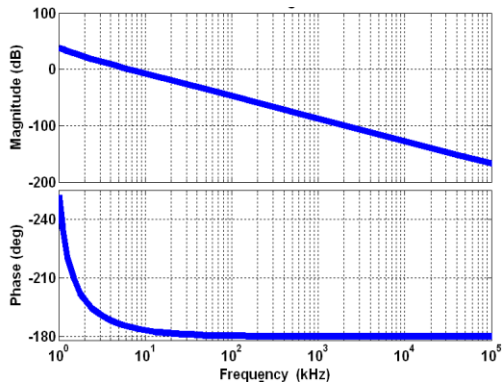
$$C_4 = (C + C_d)(L_1L_2 - M^2) + C_dR_dR_{0L}(CL_2 + C_{in}L_1 + D^2C_{in}L_2 - 2C_{in}DM)$$

$$D_4 = CL_2R_{0L} - C_d(L_1R_d + L_2R_{0L}) + C_dDR_d(2M - DL_2) + C_{in}R_{0L}(L_1 - 2DM + L_2D^2)$$

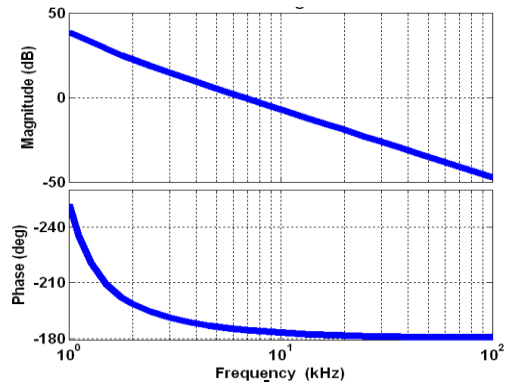
$$E_4 = C_dR_dR_{0L} - L_2D^2 - L_1 + 2MD,$$

$$F_4 = R_{0L}$$

Bode plot of control-to-output transfer function of the proposed bidirectional converter in quadratic boost mode and quadratic buck mode is given in Fig. B.2. For control-to-output transfer function components values are taken as $L_1= 291\mu\text{H}$, $L_2= 577\mu\text{H}$, $C_o=100\mu\text{F}$, $C_{in}=100\mu\text{F}$, $C=47\mu\text{F}$, $C_d=220\mu\text{F}$, $R_d=4\Omega$ for 100 kHz switching frequency. Same components used for both the modes of operations. From Fig. B. 2 it is clear that RHP zeros are completely eliminated.



(a)



(b)

Fig. B.2. Bode plots of control to output transfer function of (a) Quadratic Boost mode of operation (b) Quadratic Buck mode of operation.



APPENDIX C

The values of coefficients $A' - E'$ and $A'' - F''$ of (2.40) are given as follows:

$$A' = C_1 C_{dm} R_{odc} R_{dm} (M^2 - L_1 L_2) (V_{odc} - I_2 R_i),$$

$$B' = R_{odc} [(I_2 R_i - V_{odc})(C_1 + C_{dm})(M^2 - L_1 L_2) + C_1 C_{dm} R_i R_{dm} (1 - D)(L_1 V_{odc} + M V_{c1})],$$

$$C' = R_{odc} [C_{dm} R_{dm} (1 - D)^2 (I_1 M R_i - I_2 L_2 R_i - L_2 V_{odc}) + M(1 - D) R_i (C_1 + C_{dm}) + C_{dm} (1 - D) R_{dm} (2 I_2 M R_i - I_1 L_1 R_i - 2 M V_{odc}) + L_1 ((1 - D) R_i R_{odc} (C_{dm} + C_1) + C_{dm} R_{dm} (V_{odc} - I_2 R_i))],$$

$$D' = R_{odc} [(V_{odc} - I_2 R_i)(L_1 - 2M(1 - D) + L_2(1 - D)^2) - (1 - D) I_1 L_1 R_i + (1 - D)^2 I_1 M R_i + C_{dm} (1 - D)^2 R_{dm} R_i V_{c1} + C_{dm} (1 - D)^3 R_{dm} R_i V_{odc}],$$

$$E' = R_{odc} (V_{odc} (1 - D)^3 + V_{c1} (1 - D)^2) R_i,$$

$$A'' = C_1 C_2 C_{dm} R_{odc} R_{dm} R_i (L_1 L_2 - M^2),$$

$$B'' = \left(C_1 C_2 R_{odc} R_i + C_2 C_{dm} R_{odc} R_i + C_1 C_{dm} R_{dm} R_i \right) (L_1 L_2 - M^2) + C_1 C_{dm} (1 - D) R_{dm} R_{odc},$$

$$C'' = (C_1 + C_{dm})(L_1 L_2 - M^2)(R_i + R_{odc}(1 - D)) + C_{dm} R_{odc} R_{dm} R_i (C_1 L_1 + C_2 L_2)(1 - D)^2 + C_2 C_{dm} R_{odc} R_{dm} R_i (L_1 - 2M(1 - D)),$$

$$D'' = (R_{odc} R_i (C_2 L_2 + C_1 L_1) + C_{dm} R_i (L_2 R_{dm} + L_1 R_{odc}) - 2 C_{dm} M R_{dm} R_{odc})(1 - D)^2 - (1 - D)(C_{dm} L_1 R_{dm} R_{odc} - 2 M R_i (R_{odc} C_2 + C_{dm} R_{dm})) + C_{dm} (1 - D)^3 L_2 R_{dm} R_{odc} + L_1 R_i (C_2 R_{odc} + C_{dm} R_{dm}),$$

$$E'' = C_{dm} R_{odc} R_{dm} R_i (1 - D)^4 + L_2 R_i (1 - D)^2 - 2M(1 - D) R_i + R_i L_1 + R_{odc} (1 - D)(L_1 + (1 - D)^2 L_2 - 2((1 - D)M)),$$

$$F'' = R_{odc} (1 - D)^4 R_i.$$



APPENDIX D

The values of coefficients $A' - D'$ and $A'' - E''$ of (3.38) are given as follows:

$$A' = C_1 L_1 L_2 R_{dc} V_{C2} - C_1 L_1 L_2 I_2 R_i ,$$

$$B' = C_1 L_1 (1 - D) R_{dc} R_i V_{C2} ,$$

$$C' = L_1 R_{dc} V_{C2} - L_1 R_{dc} R_i I_2 + L_2 R_{dc} V_{C2} (1 - D)^2 - L_1 R_{dc} R_i I_1 (1 - D) - L_2 R_{dc} R_i I_2 (1 - D)^2 ,$$

$$D' = R_{dc} R_i V_{C2} (1 - D)^3 + R_{dc} R_i V_{C1} (1 - D)^2 ,$$

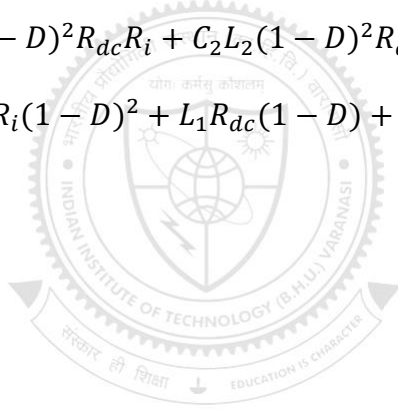
$$A'' = C_1 C_2 L_1 L_2 R_{dc} R_i ,$$

$$B'' = C_1 L_1 L_2 R_i + C_1 (1 - D) L_1 L_2 R_{dc} ,$$

$$C'' = C_1 L_1 R_{dc} R_i + C_1 L_1 (1 - D)^2 R_{dc} R_i + C_2 L_2 (1 - D)^2 R_{dc} R_i ,$$

$$D'' = L_2 R_{dc} (1 - D)^3 + L_2 R_i (1 - D)^2 + L_1 R_{dc} (1 - D) + L_1 R_i ,$$

$$E'' = R_{dc} (1 - D)^4 R_i .$$





APPENDIX E

The proposed switched qZSI topologies have high voltage gain in low shoot-through duty cycle with the same characteristic of classical qZSI such as continuous input current and common earthing of inverter bridge. The proposed switched qZSI is a modified version of classical qZSI in which inverter side inductor are switched by one auxiliary active switch and one diode. The qZSI inverter side inductor and capacitor is used for switched operation to achieve high voltage gain instead of using additional inductors or capacitors.

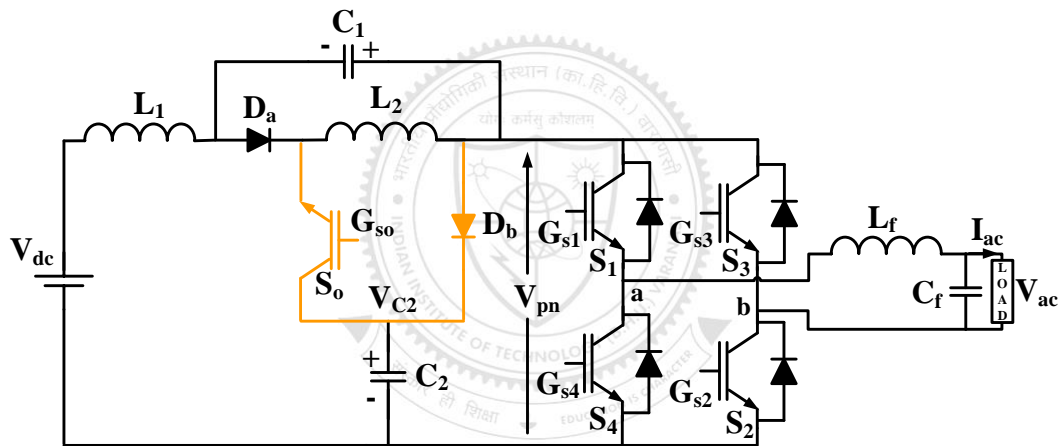


Fig. E. 1. Proposed switched qZSI

E.1. Proposed Modified Switched -qZSI

The proposed modified continuous input SBI consist of two capacitor (C_1, C_2) and two inductors (L_1, L_2) similar to classical qZSI. It is important to note that in the proposed converter, the inductor and capacitor are switched (as shown in Fig. E.1) by one auxiliary active switch and one diode.

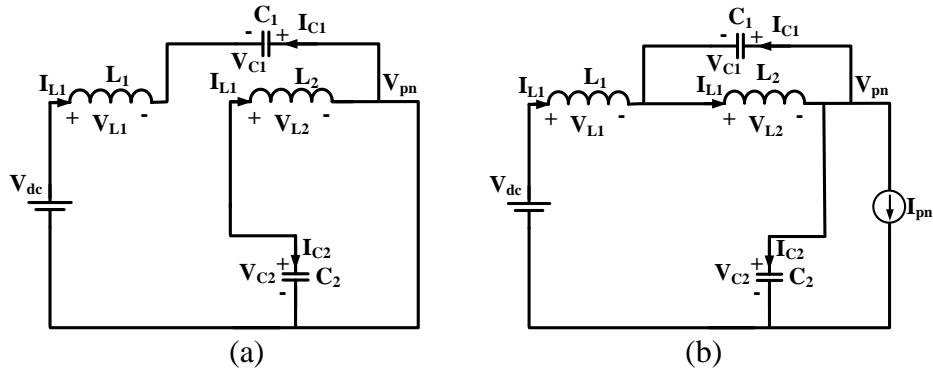


Fig. E.2. Equivalent circuit model in operating states (a) shoot-through interval (b) non-shoot-through interval

E.2. Operating Principle of the Proposed Modified Switched qZSI

The voltages across inductors L_1 and L_2 are V_{L1} , V_{L2} , respectively and V_{C1} , V_{C2} are the voltage across the capacitors. Capacitor currents are I_{C1} , I_{C2} and current through inductors are I_{L1} , I_{L2} respectively. The behaviour of the equivalent circuit in these intervals is shown in Fig. E.2 (a) and E.2 (b), respectively. In this equivalent circuit, V_{pn} is a voltage across the inverter switch and I_{pn} is a current flowing through the inverter bridge during a non-shoot-through interval.

The equivalent circuit diagram in a shoot-through mode of the interval is shown in Fig. E.2 (a). The voltage across the inductors and currents through the capacitors in the shoot-through interval are written as,

$$L_1 \frac{di_{L1}}{dt} = V_{dc} + V_{C1} \quad (\text{E.1})$$

$$L_2 \frac{di_{L2}}{dt} = V_{C2} \quad (\text{E.2})$$

$$C_1 \frac{dV_{C1}}{dt} = -I_{L1} \quad (\text{E.3})$$

$$C_2 \frac{dV_{C2}}{dt} = -I_{L2} \quad (\text{E.4})$$

The behavior of proposed inverter in a non-shoot-through mode is shown as an equivalent circuit in Fig. E.2 (b). The voltage across the inductors and current through the capacitors in the non-shoot-through interval is obtained as follows:

$$L_1 \frac{di_{L1}}{dt} = V_{dc} + V_{c1} - V_{c2} \quad (E.5)$$

$$L_2 \frac{di_{L2}}{dt} = -V_{c1} \quad (E.6)$$

$$C_1 \frac{dV_{c1}}{dt} = I_{L2} - I_{pn} \quad (E.7)$$

$$C_2 \frac{dV_{c2}}{dt} = I_{L1} - I_{pn} \quad (E.8)$$

The steady state analyses are carried out using (E.1)-(E.8). The voltage-second balance principle is applied to the inductors L_1 and L_2 over a single switching interval. By using (E.1)-(E.2) and (E.5)-(E.6) the following is obtained:

$$V_{c1} = \frac{D}{1-3D+D^2} V_{dc} \quad (E.9)$$

$$V_{c2} = \frac{1-D}{1-3D+D^2} V_{dc} \quad (E.10)$$

The switched node voltage across the inverter bridge can be written as,

$$V_{pn} = \frac{1-D}{1-3D+D^2} V_{dc} \quad (E.11)$$

Boost factor (B) is defined as,

$$B = \frac{V_{pn}}{V_{dc}} = \frac{1-D}{1-3D+D^2} \quad (E.12)$$

From (E.12) boost factor (voltage gain) can be achieved. Plot of B and G with respect to duty cycle and M is shown in Fig. E.3. The plot shows that proposed inverter gives higher gain as compared to classical ZSI, qZSI, and SBI.

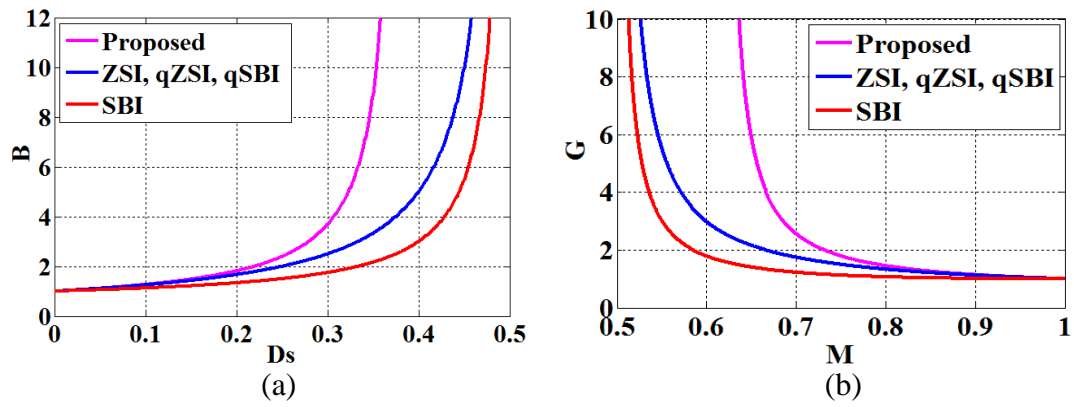


Fig. E.3. Comparison of gain factors (a) boost factor variation with D (b) peak ac gain variation with M .



APPENDIX F

In this work, active switched capacitor based two single-phase inverters are presented for improving boost capability. The proposed inverter is derived from the basic ZSI/qZSI, in which there is a possibility of the active switched capacitor which can be applied to a conventional discontinuous input current qZSI/ZSI, as well as continuous input qZSI without adding any passive elements. To enhance boost capability, the active switched capacitor is used in the conventional capacitor assisted extended switched boost ZSI (CA-ESBZSI) and diode assisted extended switched boost ZSI (DA-ESBZSI). By doing this, no extra passive components are increased, i.e., only one diode and one switch is additionally used. The proposed inverters are suitable for low or medium voltage DC microgrid application where high AC voltage gain is required. The capacitor assisted extended switched boost Z-source inverter is shown in Fig. F.1(a). The diode assisted extended switched boost ZSI is shown in Fig. F.1(b).

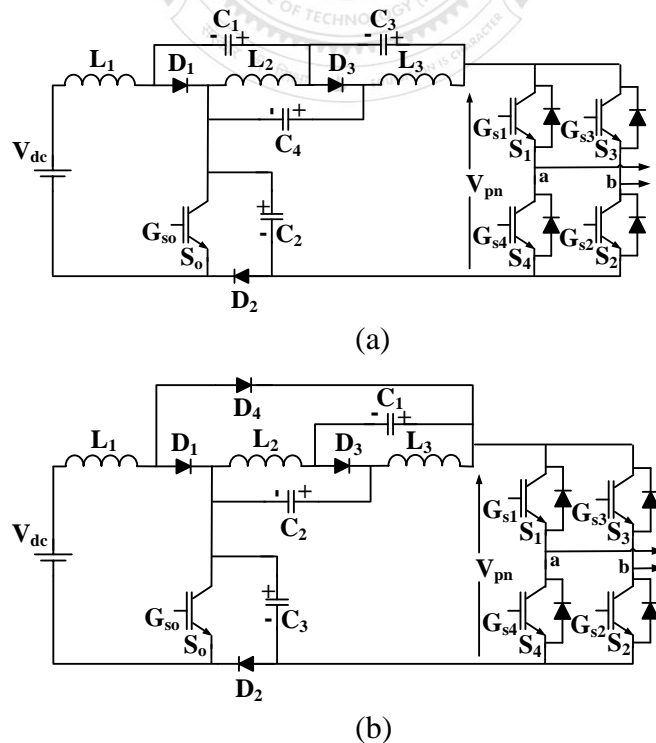


Fig. F.1. Proposed extended switched boost ZSI (a) Capacitor assisted extended switched boost ZSI (b) Diode assisted extended switched boost ZSI

F.1. Capacitor Assisted Extended Switched Boost ZSI

The voltages across inductors L_1 , L_2 and L_3 are V_{L1} , V_{L2} and V_{L3} respectively and V_{C1} , V_{C2} , V_{C3} and V_{C4} are the voltage across the capacitors. The capacitor voltages V_{C1} , V_{C3} , V_{C4} are equal and inductors current are also equal. The current through inductors are I_{L1} , I_{L2} , I_{L3} and capacitors currents are I_{C1} , I_{C2} , I_{C1} . The behaviour of the equivalent circuit is shown in Fig. F.2 (a) and F.2 (b), respectively.

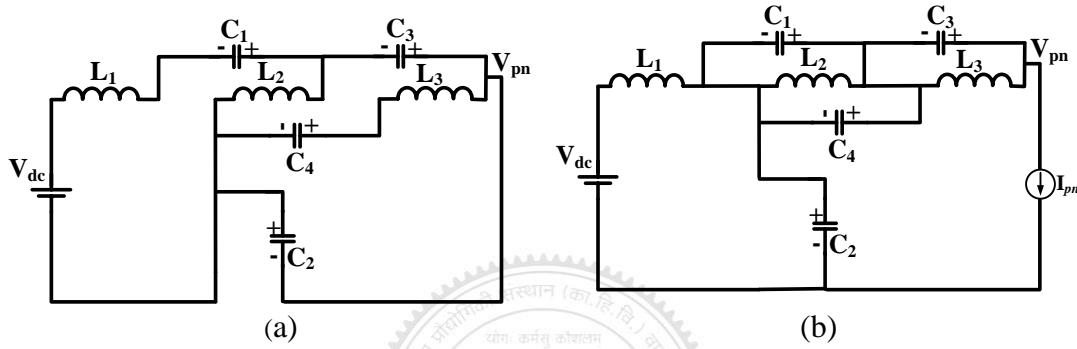


Fig. F.2. Extended capacitor assisted switched boost ZSI operation (a) Equivalent circuit model in operating in shoot-through interval (b) Equivalent circuit model in non-shoot-through interval.

During Shoot-through interval following is obtained.

$$L_1 \frac{di_1}{dt} = V_{dc} + V_{c1} + V_{c2} + V_{c3} \quad (F.1)$$

$$L_2 \frac{di_2}{dt} = V_{c2} + V_{c3} \quad (F.2)$$

$$L_3 \frac{di_3}{dt} = V_{c2} + V_{c4} \quad (F.3)$$

During non-shoot-through interval, following equations are obtained.

$$L_1 \frac{di_1}{dt} = V_{dc} - V_{c2} \quad (F.4)$$

$$L_2 \frac{di_2}{dt} = -V_{c2} = -V_{c4} \quad (F.5)$$

$$L_3 \frac{di_3}{dt} = -V_{c3} \quad (F.6)$$

By utilizing the shoot-through and non-shoot-through interval equations, the steady state modeling is carried out. The steady state analyses are carried out using shoot-

through and non shoot-through equations. The voltage- second balance principle is applied to the inductors L_1 , L_2 and L_3 over a single switching interval. By using (F.1)-(F.6), following is obtained:

$$V_{c1} = V_{c3} = V_{c4} = \frac{D}{1-4D+2D^2} V_{dc}, \quad V_{c2} = \frac{1-2D}{1-4D+2D^2} V_{dc},$$

$$V_{pn} = V_{c1} + V_{c2} + V_{c3} = \frac{1}{1-4D+2D^2} V_{dc}$$

Boost factor (B) is defined as, $B = \frac{V_{pn}}{V_{dc}} = \frac{1}{1-4D+2D^2}$ (F.7)

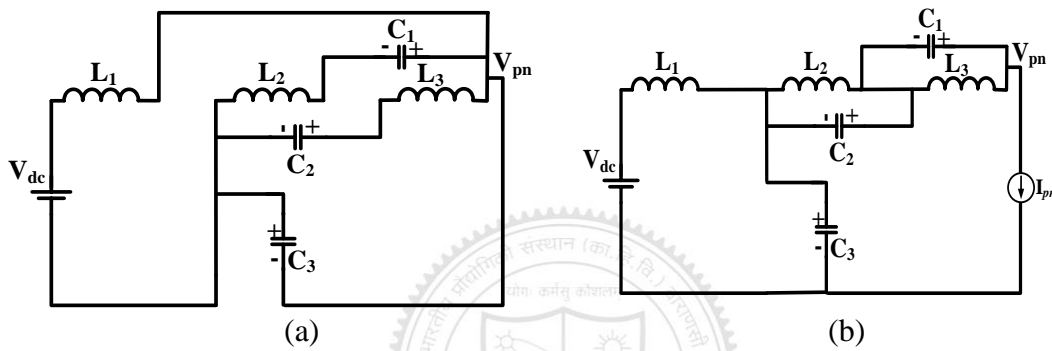


Fig. F.3. Extended diode assisted switched boost ZSI operation (a) Equivalent circuit model in operating in shoot-through interval (b) Equivalent circuit model in non-shoot-through interval.

F.2. Diode Assisted Extended Switched Boost ZSI

The voltages across inductors L_1 , L_2 and L_3 are V_{L1} , V_{L2} and V_{L3} respectively and V_{c1} , V_{c2} and V_{c3} are the voltage across the capacitors. The current through inductors are I_{L1} , I_{L2} I_{L3} and capacitors currents are I_{c1} , I_{c2} , I_{c3} . The capacitor voltages V_{c1} , and V_{c2} are equal. The behaviour of the equivalent circuit is shown in Fig. F.3 (a) and F.3 (b), respectively.

During Shoot-through interval, following is obtained.

$$L_1 \frac{di_1}{dt} = V_{dc} + V_{c3} \quad (F.8)$$

$$L_2 \frac{di_2}{dt} = V_{c1} + V_{c3} \quad (F.9)$$

$$L_3 \frac{di_3}{dt} = V_{c2} + V_{c3} \quad (\text{F.10})$$

During non-shoot-through interval, following equations are obtained.

$$L_1 \frac{di_1}{dt} = V_{dc} - V_{c3} \quad (\text{F.11})$$

$$L_2 \frac{di_2}{dt} = -V_{c2} \quad (\text{E.12})$$

$$L_3 \frac{di_3}{dt} = -V_{c1} \quad (\text{F.13})$$

Shoot-through and non-shoot-through interval equations are utilized for the steady state modeling. The voltage-second balance principle is applied to the inductors L_1 , L_2 and L_3 over a single switching interval. By using (F.8)-(F.13) the following is obtained:

$$V_{c1} = V_{c2} = \frac{D}{(1-2D)^2} V_{dc}, \quad V_{c3} = \frac{1}{1-2D} V_{dc},$$

$$V_{pn} = V_{c1} + V_{c2} + V_{c3} = \frac{1}{(1-2D)^2} V_{dc}$$

Boost factor (B) is defined as, $B = \frac{V_{pn}}{V_{dc}} = \frac{1}{(1-2D)^2}$ (F.14)

This boost factor property can also be described as quadratic boost factor of ZSI/qZSI.

The simple boost PWM technique has constraints of $(D + M) \leq 1$, so the relationship between the ac peak gain and M is as follows:

$$G = M \cdot B = \frac{M}{(2M-1)^2} \quad (\text{F.15})$$

From (F.14), it is clear that the proposed inverter gives higher ac voltage gain as compared to conventional extended boost ZSI [10]. Fig. F.4 shows the comparisons of gain plot.

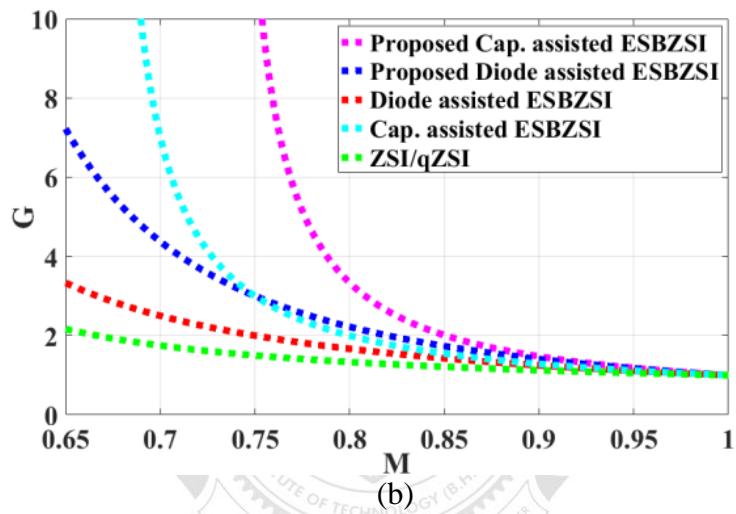
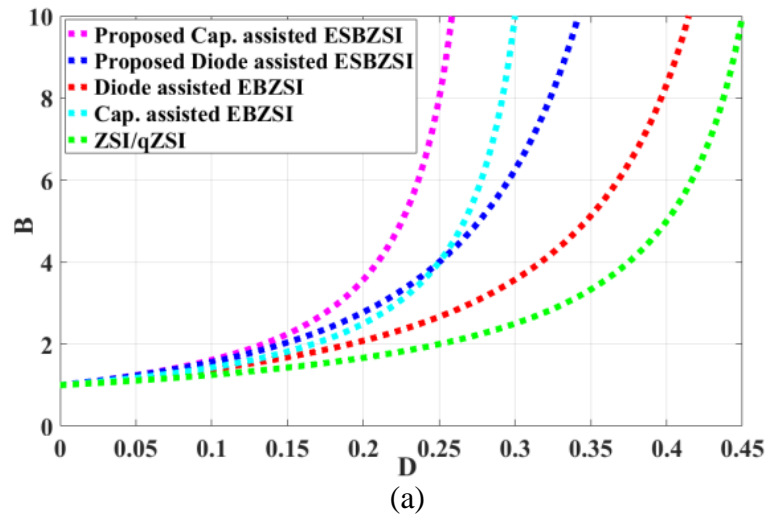


Fig. F.4. Gain plot comparisons (a) Boost factor plot (b) AC gain plot

